JOURNAL OF MATERIALS SCIENCE 21 (1986) 3653–3660

Effect of transition elements on the properties of MC carbides in IN-100 nickel-based superalloy

YOSHINORI MURATA, KIYOSHI SUGA, NATSUO YUKAWA
Department of Production Systems Engineering, Toyohashi University of Technology, Hibarigaoka, Tempaku-cho, Toyohashi 440, Japan

The effect of nine transition elements on the morphology, distribution and composition of MC carbides (MCs) in a nickel-base superalloy, IN-100, was investigated by differential thermal analysis (DTA), microstructural observation and X-ray microanalysis. The doping with tantalum, tungsten and molybdenum caused a significant change in the morphology and distribution of MCs as well as the profile of DTA curve of IN-100. The compositions of the MC in IN-100 were TiC and $(Ti_{0.80}Mo_{0.17}V_{0.03})C$, and the doping with niobium, tantalum and tungsten changed significantly the composition of MC. On the other hand, the doping with chromium, vanadium, hafnium and zirconium scarcely changed the composition. In addition to TiC and (Ti, Mo, V) C, zirconium- and hafnium-rich MCs were found in the zirconium- and hafnium-doped alloys, respectively. The effect of the dopants on the composition of MCs could be explained by a relationship between the metallic radius and the free energy of formation for the MC.

1. Introduction

In most nickel-base superalloys, MC forms during solidification and it exists mainly at and around the grain boundaries. The mechanical properties of the cast nickel-base superalloys are affected strongly by the morphology and distribution of the carbide [1–3]. It is known that the so-called script-type MC in the grain boundaries deteriorate the tensile ductility [1], since it provides not only the crack-initiation site, but also the crack-propagation path for the failure [3]. Under a constant condition of solidification, the morphology and distribution of MC are varied with the alloy composition, which also affects the composition of MC. Therefore, the properties such as the morphology of MC depend on its composition. In the superalloys, the MCs contain several kinds of transition elements. For instance, they are reported to be $(Ti_{0.53}Nb_{0.31}W_{0.16})C$ in Mar-M 200 (at %: 0.69 C, 10.79 Cr, 10.31 Co, 2.54 Ti, 11.04 Al, 3.90 W, 0.05 B, 0.03 Zr, bal.Ni) [4], and $(Ti_{0.77-0.81}Mo_{0.18-0.21})C$ in Udimet 700 (at %: 0.32 C, 16.09 Cr, 17.20 Co, 3.08 Mo, 3.86 Ti, 8.81 Al, 0.12 B, bal.Ni) [5]. The transition elements operating as the MC former are also the strengthening elements of the γ matrix precipitated γ' phase in the nickel-base superalloys. Therefore, from the alloy design viewpoint, it is important to know the composition of MC exactly on the basis of a fundamental factor.

The MC usually transforms into the $M_{23}C_6$ carbide ($M_{23}C_6$) after exposure at high temperatures, as a result of the reaction between MC and γ: MC + $\gamma \rightarrow M_{23}C_6 + \gamma'$ [6, 7]. Also, the $M_{23}C_6$ transforms into the M_6C carbide (M_6C), if a superalloy contains a large amount of tungsten [4]. It has been reported that since $M_{23}C_6$ and M_6C contain large amounts of chromium, the surroundings of these carbides become chromium-depleted regions, and give the initiation points of stress-corrosion cracking [8]. Furthermore, the $M_{23}C_6$ in a cellular form and the Widmanstätten M_6C at grain boundaries is reported to impair the ductility and rupture lives, while blocky and less continuous $M_{23}C_6$ improved the rupture lives [9]. As the result of the reaction mentioned above, it is considered that the distribution and morphology of $M_{23}C_6$ and M_6C secondarily formed depend largely on those of MC primarily formed. Therefore, it is important to control the morphology and distribution of MC in order to develop the nickel-base superalloys with superior mechanical properties.

The purpose of this study is to reveal the effects of the various transition elements on the properties of MCs, in particular, on their morphology, distribution and composition. IN-100 alloy was selected for this investigation. This alloy is one of the most well-known alloys for the parts of jet-engines, and their solidification sequence has been recently elucidated by the authors [10].

2. Experimental procedure

A heat of IN-100 alloy used as the mother alloy in this study was provided by the Ishikawajima-harima Heavy Industry Co. Ltd in the form of a cast bar of 80 mm in diameter. Table I shows the composition and the Aerospace Material Specification (AMS) of this alloy.

In this study, the doping method was employed to

0022–2461/86 $03.00 + .12

TABLE I Chemical composition of IN-100 used in the present experiment, and the Aerospace Material Specification (AMS)

	Cr	Co	Mo	Ti	Al	V	C	B	Zr	Ni	N	O
at%	9.23	12.63	1.67	5.40	11.09	0.81	0.72	0.075	0.022	bal.	0.0023	0.0030
wt%	8.85	13.73	2.95	4.77	5.52	0.76	0.16	0.015	0.037	bal.	0.0006	0.0009
AMS (wt%)	8 ~ 11	13 ~ 17	2 ~ 4	4.5 ~ 5.0	5 ~ 6	0.7 ~ 1.2	0.15 ~ 0.2	0.01 ~ 0.02	0.03 ~ 0.09	bal.	—	—

investigate the effect of individual transition elements on the properties of MC. This method consists of the following three steps. Firstly, the specific transition element was doped into the mother alloy by using a tri-arc furnace [11]. Secondly, DTA (differential thermal analysis) was performed on both the mother alloy and the doped alloys. Thirdly, the distribution, morphology and composition of MC were examined on the samples after DTA.

Doped alloys were prepared by adding each of the transition elements of 0.0015 mole to the mother alloy of 0.010 kg in weight. This amount of doping corresponds to approximately 0.81 at%. Button ingots of these alloys were melted by using a tri-arc furnace in a purified argon atmosphere. As shown in Table II, the nine transition elements were selected as the dopants. They belong to the groups IVa, Va and VIa in the 4th, 5th and 6th rows of the periodic table. Since titanium, molybdenum and vanadium of the nine elements are the constituent elmenents of IN-100, their amounts of doping were determined so that the total amount of the element did not greatly exceed the upper limit of the alloy composition defined by the specification.

A series of experiments with IN-100 and the doped alloys was performed by the DTA, microstructural observation using the scanning electron microscope (SEM), X-ray microanalysis (EPMA) and X-ray diffraction. The DTA was carried out by the use of a DT-1500H system (Shinku-Riko Ltd) under a purified argon atmosphere. The sample of about 2×10^{-4} kg was kept in a molten state at 1723 K (1450° C) for 900 sec, and then the DTA curve was obtained during cooling at a rate of 0.83 K sec^{-1} (5° C min^{-1}). Alumina powder was used for a reference material. After DTA experiment, the samples were etched electrolytically either to emboss the MC on the sample or to extract the MC from the sample. The electrolyte used was a 10% hydrochloric acid–1% tartaric acid–methanol solution. The distribution of MC in the etched samples and the morphology of the extracted MC were observed using a SEM (Hitachi, X650 system). To determine the chemical composition of the extracted MC, the electron probe microanalysis was carried out by using a WDX (Hitachi Ltd) and an EDX (Horiba Ltd) spectrometer with a spot size of 1000 nm.

TABLE II Nine elements selected as the dopants

Row	Group		
	IVa	Va	VIa
4	Ti	V	Cr
5	Zr	Nb	Mo
6	Hf	Ta	W

3. Results

Fig. 1 shows a typical SEM photograph of IN-100 obtained in this study. The white phase is MC in this figure. The solidification structure of IN-100 consists of γ, γ', MC and M_3B_2 phases, and these phases are formed by six reactions [10]. As shown in Fig. 2, the DTA curve of IN-100 exhibits six exothermic peaks. The peaks P_2 and P_3 are associated with the formation of dendritic and interdendritic MCs, respectively [10]. The dendritic MC denoted by MC(D) occurs between primary dendrite arms, while the interdendritic MC denoted by MC(ID) exists between each dendrite [12]. Peaks P_4, P_5 and P_6 are related to the formation of $\gamma + \gamma'$ eutectic phase, γ' precipitates in the γ matrix and $\gamma + M_3B_2$ eutectic phase, respectively. Peaks P_6 and P_5 were supposed to be overlapped in this case, because the temperature difference between the two peaks was only a few Kelvin, and also the peak P_5 was very diffuse due to the reaction in a solid.

DTA curves of the doped alloys are shown in Fig. 3. In these curves, we focused attention on peaks P_2 and P_3, since the effect of the doping elements on the occurrence of MCs appeared mainly on these two peaks. The measured DTA curves of the doped alloys were classified into three types according to the differences in the appearance of peaks P_2 and P_3. Type I was observed in titanium-, vanadium-, chromium-, zirconium-, niobium-, and hafnium-doped alloys. The DTA curves had almost the same features as that of IN-100 where peaks P_2 and P_3 show a clear separation. Peak P_7 observed in zirconium-doped alloy was due to the occurrence of the intermetallic compound Ni_7Zr_2. This compound is a eutectic phase formed at grain boundaries [13]. On the other hand, type II was observed in the tungsten- and molybdenum-doped alloys where peaks P_2 and P_3 did not separate ($P_{2\text{-}3}$).

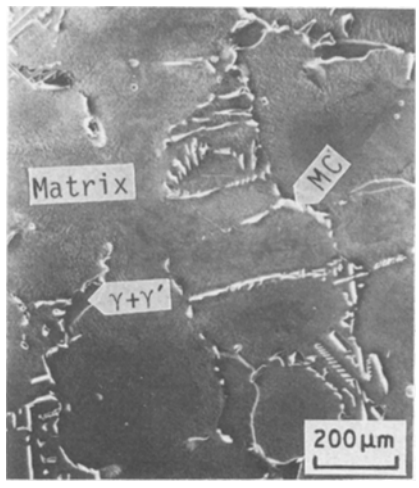

Figure 1 A SEM photograph of IN-100 observed after DTA.

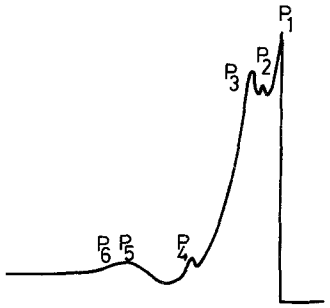

Figure 2 A DTA curve of IN-100. P_1: L → γ, 1605 K, P_2: L → γ + MC(D), 1589 K. P_3: L → γ + MC(ID), 1580 K, P_4: L → γ + γ', 1537 K. P_5: γ → γ', P_6: L → γ + M_3B_2, 1509 K.

For type III observed in a tantalum-doped alloy, the three peaks P_1, P_2 and P_3 merged into one peak ($P_{1\text{-}2\text{-}3}$). As is shown in Fig. 4, each temperature of the DTA peaks of doped alloys was very similar to those of IN-100 except for the chromium-doped alloy. In the chromium-doped alloy, every peak temperature is lower by approximately 30 K compared with IN-100, and peak P_4, which was related to the γ + γ' eutectic reaction, was not observed. The temperatures of the $P_{2\text{-}3}$ peak in type II and the peak $P_{1\text{-}2\text{-}3}$ in type III were close to the peak temperature of P_1 and P_2 in IN-100, respectively. The MC occurs at higher temperature in types II and III than in IN-100.

The difference existing in the DTA profiles was owing to the difference in the distribution of MC. Typical SEM photographs are given in Fig. 5 to show the distribution of MC in doped alloys. In the alloys of the type I from (a) to (f), the MCs were mainly observed in the interdendritic region. The distribution of MC in type I was similar to that in IN-100 (see Fig. 1). On the other hand, in molybdenum-, tungsten-, and tantalum-doped alloys the MCs were distributed more homogeneously than in IN-100. In other words, for those alloys, in which peaks P_2 and P_3, or P_1, P_2 and P_3 merged into one peak, the MCs are dispersed more homogeneously.

The morphology of MCs in the nickel-base superalloys has been described by many investigators [2, 14–16]. It has been reported that their shape looks like "Chinese script" in the case of sectional observation of the specimen, but appears octahedral or herringbone-like in the electrolytically deep-etched specimen. In our previous study [10], MCs were extracted electrolytically from IN-100, and classified into three groups according to their shape, that is, blocky, lattice-like and flaky. In this study, the same technique was employed and these three kinds of morphology were observed in all the alloys except for the zirconium-, hafnium-, and tantalum-doped alloys. In the zirconium- and hafnium-doped alloys, besides these three kinds of morphology, serrated-arrow-like MC was observed as mentioned later. Fig. 6 shows the typical morphology of MC extracted from some alloys of types I to III. Blocky carbide in types I to III had an octahedral shape. Lattice-like carbide in type I had relatively fine and long arms, intersecting at right angles to each other. On the other hand, those in type II had relatively thick and short arms. Furthermore, they had relatively large heads of octahedral shape,

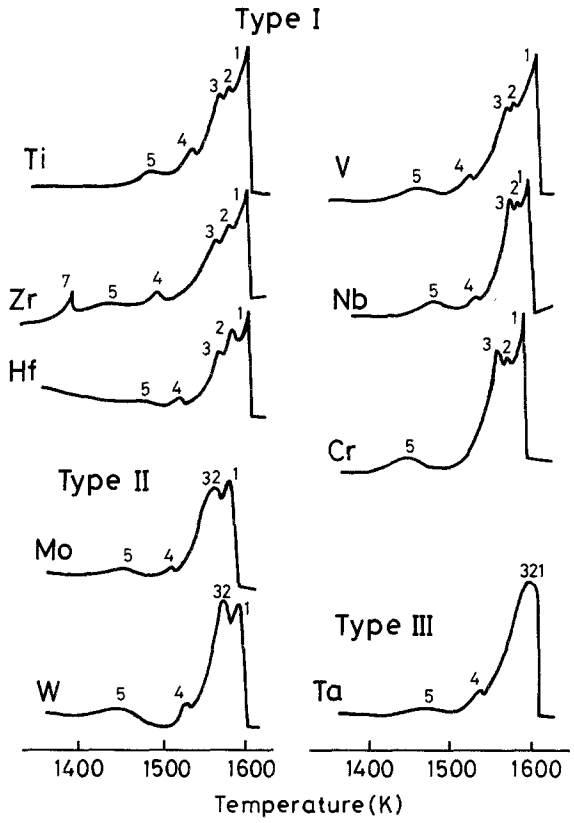

Figure 3 DTA curves of the doped alloys.

and few crossed arms. This tendency in the morphology of lattice-like carbide became more pronounced in type III. Little difference was observed in the morphology of flaky carbides in types I and II, but the amount of this carbide was rather less in type II than in type I. On the other hand, no flaky carbide was found in the tantalum-doped alloy. This morphological change is directly related to the change in the distribution of MC as shown in Fig. 5.

Fig. 7 shows the result of X-ray microanalysis (WDX) on carbon and nitrogen of the MC extracted from IN-100. Nitrogen was not found in the MC, though the existence of Ti(C,N) has been reported in a heat of IN-100 [17]. However, the present result is reasonable since IN-100 used in this study contains only 23 p.p.m. in atomic nitrogen (see Table I). In Table III, the compositions of extracted MC are summarized for each of three kinds of morphology. In IN-100, the composition of blocky carbides having octahedral shape was practically pure TiC, and lattice-like and flaky carbides were $(Ti_{0.78}Mo_{0.18}V_{0.04})C$ and $(Ti_{0.82}Mo_{0.15}V_{0.03})C$, respectively. The latter two types were considered to be almost the same composition.

The effect of dopants on the composition of MC could be classified into the following three groups. Titanium, vanadium, chromium and molybdenum belonged to the first group. Niobium, tantalum and tungsten belonged to the second group, and the third group contained zirconium and hafnium. In the first group, the composition of MC was scarcely changed by the doping of titanium, vanadium, chromium and molybdenum, because these elements were constituents of IN-100. However, niobium, tantalum and tungsten belonging to the second group changed remarkably the composition of MC in IN-100, as can

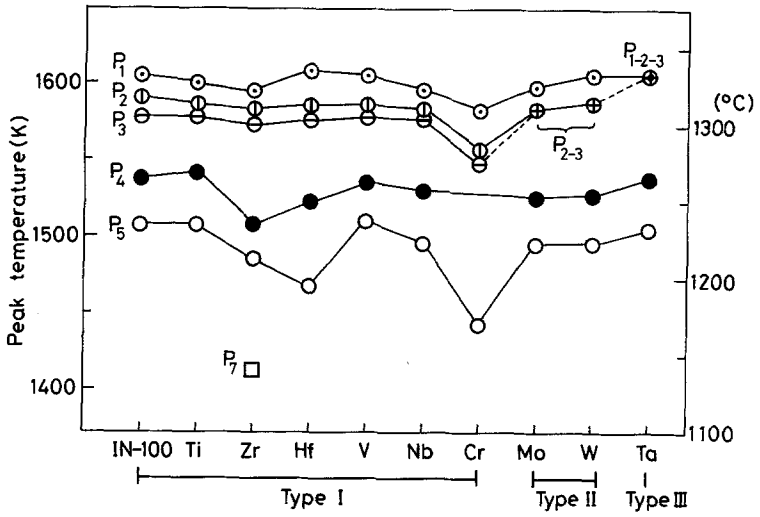

Figure 4 DTA peak temperatures of IN-100 and doped alloys.

be seen in Table III. In the niobium-, tantalum- and tungsten-doped alloys, the blocky carbide had the similar composition to the lattice-like and flaky carbide. The MC in the niobium- and tantalum-doped alloy contained doped element of about 30 at % in the metal part, respectively. Moreover, in these doped alloys, titanium and molybdenum contents of MC are lower than those in IN-100. In tungsten-doped alloy, MC contained about 10 at % W as metal atoms, and the sum of the amount of tungsten and molybdenum was about 20 at %, which was nearly equal to that of molybdenum in MC in the molybdenum-doped alloy. This implies that molybdenum and tungsten behave similarly for the formation of MC, and hence

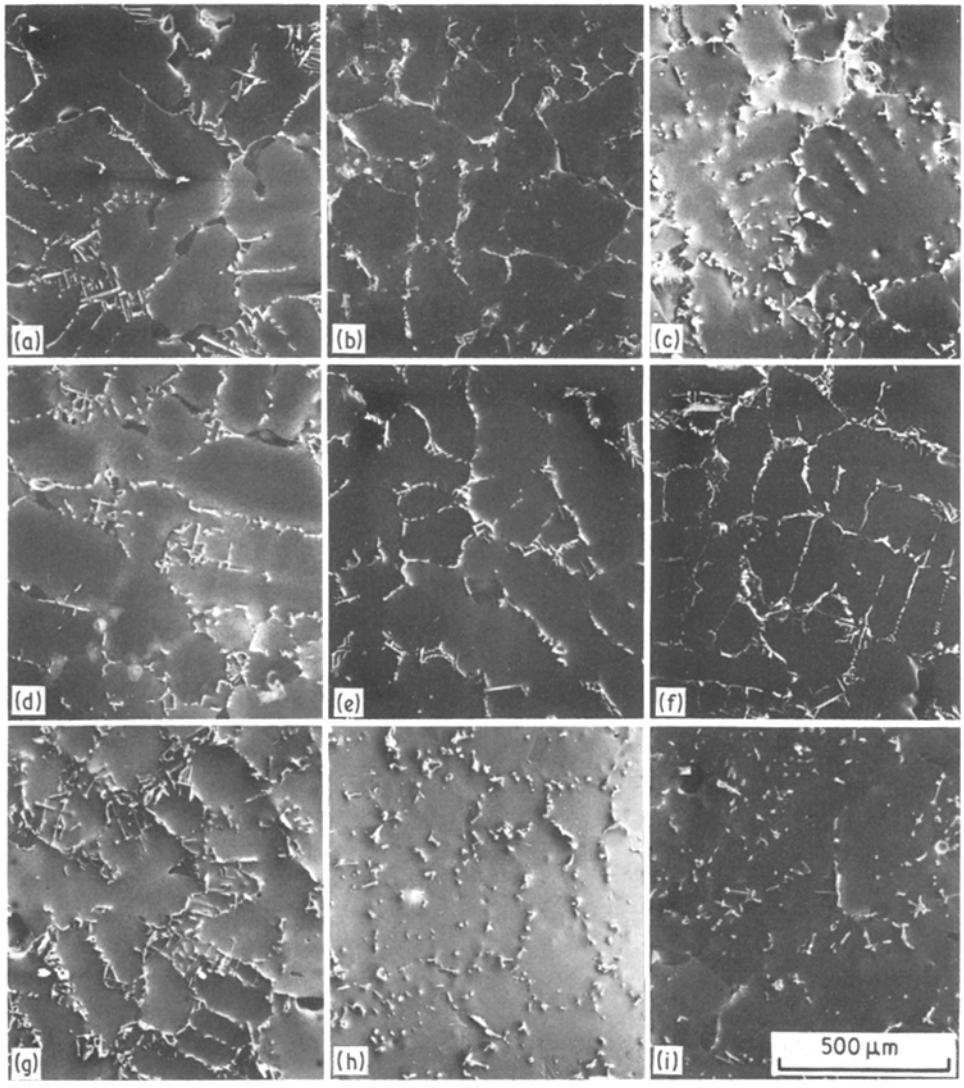

Figure 5 Typical SEM photographs showing MC carbide distribution in the doped alloys. (a) Titanium doped, (b) zirconium doped, (c) hafnium doped, (d) vanadium doped, (e) niobium doped, (f) chromium doped, (g) molybdenum doped, (h) tungsten doped, (i) tantalum doped.

TABLE III Chemical composition of MC carbides extracted from IN-100 and the doped alloys*

Doping element	Blocky (Octahedron)	Lattice-like	Flaky	Serrated-arrow-like
no (IN-100)	TiC	$(Ti_{0.78}Mo_{0.18}V_{0.04})C$	$(Ti_{0.82}Mo_{0.15}V_{0.03})C$	–
Ti	TiC	$(Ti_{0.78}Mo_{0.18}V_{0.04})C$	$(Ti_{0.78}Mo_{0.18}V_{0.04})C$	–
Zr	$(Ti_{0.97}Mo_{0.03})C$	$(Ti_{0.77}Mo_{0.19}V_{0.04})C$	$(Ti_{0.77}Mo_{0.18}V_{0.05})C$	$(Zr_{0.92}Ti_{0.08})C$
Hf	$(Ti_{0.93}Hf_{0.04}Mo_{0.03})C$	$(Ti_{0.76}Mo_{0.19}V_{0.05})C$	$(Ti_{0.68}Mo_{0.19}V_{0.05}Cr_{0.05}Hf_{0.03})C$	$(Hf_{0.80}Ti_{0.14}Zr_{0.06})C$
V	TiC	$(Ti_{0.78}Mo_{0.17}V_{0.05})C$	$(Ti_{0.75}Mo_{0.18}V_{0.07})C$	–
Nb	$(Ti_{0.92}Nb_{0.08})C^{\dagger}$	$(Ti_{0.59}Nb_{0.29}Mo_{0.12})C$	$(Ti_{0.58}Nb_{0.31}Mo_{0.11})C$	–
Ta	$(Ti_{0.60}Ta_{0.36}Mo_{0.04})C$	$(Ti_{0.66}Ta_{0.27}Mo_{0.07})C$	–	–
Cr	$(Ti_{0.80}Mo_{0.15}V_{0.03}Cr_{0.02})C$	$(Ti_{0.82}Mo_{0.15}V_{0.03})C$	$(Ti_{0.85}Mo_{0.15})C$	–
Mo	$(Ti_{0.81}Mo_{0.16}V_{0.03})C$	$(Ti_{0.76}Mo_{0.21}V_{0.03})C$	$(Ti_{0.75}Mo_{0.22}V_{0.03})C$	–
W	$(Ti_{0.76}Mo_{0.11}W_{0.10}V_{0.03})C$	$(Ti_{0.76}Mo_{0.12}W_{0.09}V_{0.03})C$	$(Ti_{0.76}Mo_{0.13}W_{0.08}V_{0.03})C$	–

*Carbon content was calculated based on fifty carbon atoms for every fifty metal atoms.
†The composition was scattered, ranging from $(Ti_{0.75}Nb_{0.25})C$ to $(Ti_{0.95}Nb_{0.05})C$.

molybdenum and tungsten are the interchangeable elements in MC. The effect of zirconium and hafnium on the composition of MC was different from the other seven elements mentioned above. Their compositions of blocky, lattice-like and flaky carbides were similar to those in IN-100. However, in addition to these three kinds of MC, $(Zr_{0.92}Ti_{0.08})C$ in zirconium-doped alloy and $(Hf_{0.80}Ti_{0.14}Zr_{0.06})C$ in hafnium-doped alloy were observed, as shown in Table III. The morphology of the zirconium- and hafnium-rich MCs is shown in Fig. 8, and it is designated as serrated-arrow-like shape. These effect of the doped elements on the composition of MC is discussed in a later section.

4. Discussion

Every transition element used in this study forms a monocarbide except for chromium. Of these elements, hafnium and zirconium in group IVa of the periodic table may form MC most easily, since the free energies of formation for HfC and ZrC are larger than those for other MC. However, no ZrC was found in the IN-100 in spite of the existence of a small amount of

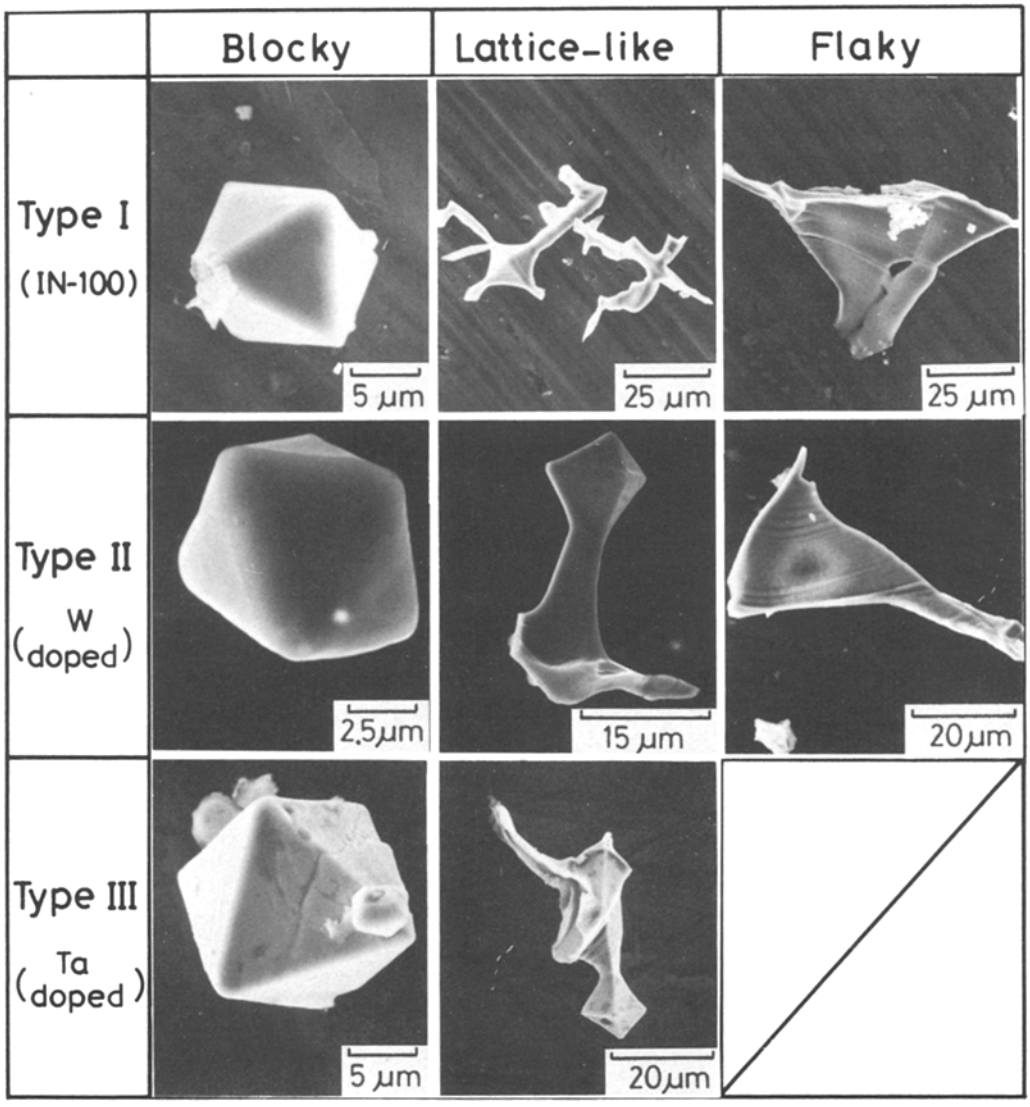

Figure 6 Typical morphology of MC carbides extracted from the alloys of three types.

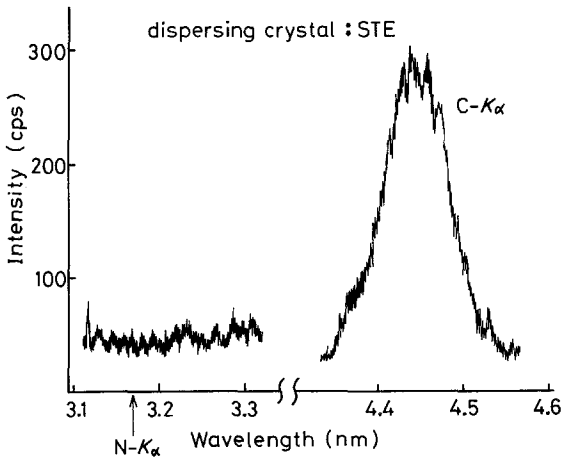

Figure 7 The result of X-ray microanalysis of the MC carbides extracted from IN-100 alloy.

zirconium. Therefore, although we must consider the properties of MC on the basis of their composition, neither the magnitude of free energy of formation for MC nor the location of the doping elements in the periodic table could explain the effect of dopants upon the composition of MCs.

Fig. 9 shows the relationship between the metallic radius and Gibbs free energy of formation for the MCs of each transition element. The data on the metallic radius and the free energy were taken from Teatum *et al.* [18] and Hultgren *et al.* [19], respectively. The value of free energy for MoC was taken from Browning and Emmett [20] and Kempter [21]; these data for MoC were obtained at 950 K. However, the value is assumed to be nearly equal to that obtaiend at 1500 K, because in most transition elements the free energy of formation for MC at 950 K is very close to that at 1500 K [19]. As chromium does not form MC, the free energy of formation for Cr_3C_2 was employed [19]. The effect of dopants on the composition of MC could be explained by the figure. As both niobium and tantalum have almost the same metallic radius and free energy as titanium (see Fig. 9), these two elements are considered to be substituted easily for titanium. This is consistent with the fact that in the niobium- and tantalum-doped alloys about 30% of the metallic atoms consisted of the doping element in MC, as shown in Table III. On the other hand, although the metallic radius of the molybdenum and tungsten is smaller than that of titanium, the amount of difference is not significant. Consequently, in the molybdenum-doped alloy, the metal elements of MC contain about 20 at % Mo. Furthermore, as the metallic radius of molybdenum is similar to that of tungsten, these two elements are interchangeable with each other. Therefore, the sum of molybdenum and tungsten contents in MC is about 20 at % in the tungsten-doped alloy. It is noticed that both molybdenum and tungsten play an important role for the MC formation through the lattice constriction. In fact, the measured lattice parameter of MC extracted from IN-100 was 0.4136 nm, which is smaller than that of TiC, 0.432 80 nm [22]. This lattice constriction may result in a strong atomic bonding in MC due to the increase in the overlapping of the electron wavefunction.

The metallic radii of zirconium, hafnium, vanadium and chromium differ greatly from that of titanium. For this reason, even in the alloy doped with these four elements, the titanium-rich MC contains only a small amount of them. However, since ZrC and HfC have a large free energy of formation for MC compared with that for TiC, the zirconium-rich (Zr, Ti) C in the zirconium-doped alloy, and the hafnium-rich (Hf, Zr, Ti) C in the hafnium-doped alloy were found together with TiC and (Ti, Mo, V) C, as is shown in Table III.

In the zirconium-doped alloy, the new peak P_7 was observed at very low temperature in the DTA curve. It was probably related to the formation of the Ni_7Zr_2 intermetallic compound which existed at grain boundaries. Zirconium has a significant low solubility in the nickel-base superalloys [23], and hence zirconium is likely to be enriched in the residual liquid as the solidification proceeds.

An octahedral shape of MC indicates that the MC grow by deposition of the {1 1 1} atomic plane. In the MC having NaCl structure, it is obvious that {1 1 1} planes consist of the alternate stacking with the metal and carbon layers. The Nb–Ti and Ta–Ti systems form a complete solid solution above 1158 K [24]. Therefore, tantalum and niobium are considered to form easily {1 1 1} metal planes with titanium, and to be highly soluble in TiC and (Ti, Mo) C in IN-100. As mentioned above, the distance between metal atoms in the {1 1 1} plane tends to constrict, probably owing to the strength of atomic bonding. The change of the

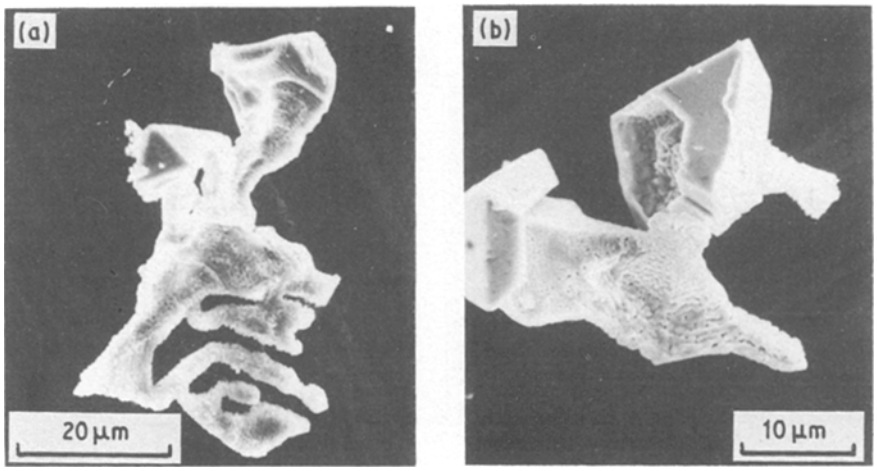

Figure 8 Morphology of serrated-arrow-like carbide. (a) Zirconium-rich MC, (b) hafnium-rich MC.

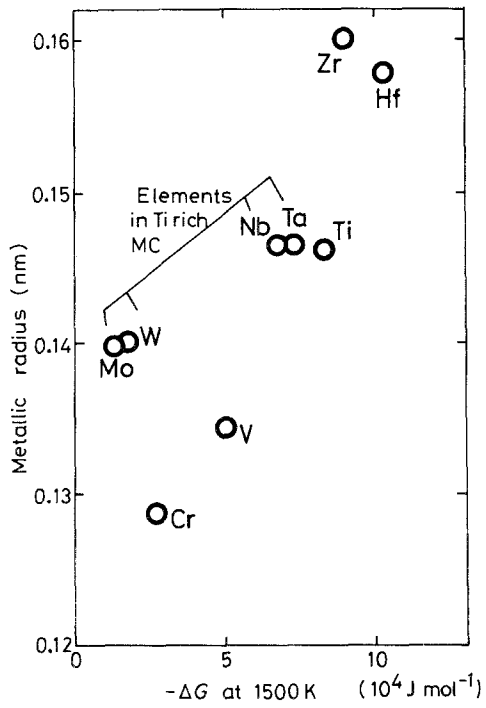

Figure 9 The relationship between the metallic radius and the Gibbs free energy at 1500 K for the MC-carbide formation.

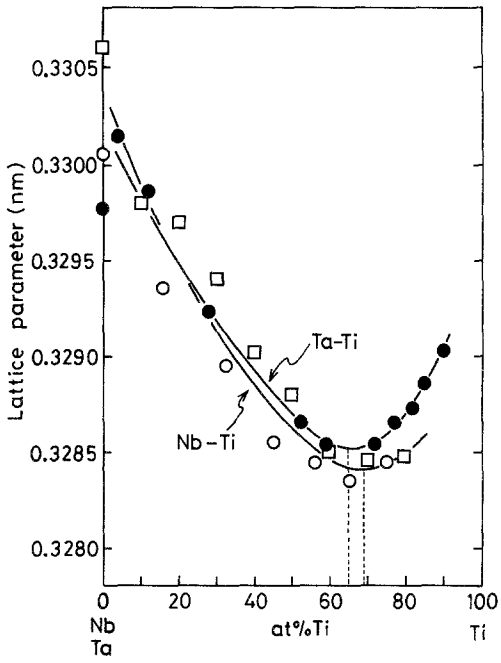

Figure 10 Change of the lattice parameter of the solid solution in Ti–Nb and Ti–Ta systems. □, Nb–Ti [25]; ○, Nb–Ti, ●, Ta–Ti [26].

lattice-parameters in the Nb–Ti and Ta–Ti systems is shown in Fig. 10. These were taken from Hansen *et al.* [25] and Rudy [26]. The two systems have a minimum value of the interatomic distance in each solid solution. As the lattice parameter of pure titanium is only a little different from pure niobium and tantalum, the composition of MC containing tantalum and niobium may be changed by the alloy composition. For example, in Inco 713C (at %: 0.55 C, 13.95 Cr, 2.44 Mo, 0.93 Ti, 12.98 Al, 1.57 Nb, 0.04 B, 0.03 Zr, bal.Ni) containing a large amount of niobium, the composition of primary MC is reported to be $(Nb_{0.77}Ti_{0.23})C$ [16]. However, the minimum lattice parameter occurs at about 30 at % Nb in the Nb–Ti system, and at about 35 at % Ta in the Ta–Ti system. Their concentrations agree with the composition of MC in the niobium- and tantalum-doped alloys. Therefore, the concentration of niobium and tantalum at the minimum lattice parameter probably determines the composition of MC in the niobium- and tantalum- doped alloys.

The DTA curves are classified into three types according to the difference in the appearance of peaks P_1, P_2 and P_3. The distribution of MC in IN-100 can be predicted to some extent by using the profiles of DTA curves. In both type II, in which peaks P_2 and P_3 overlap, and type III, in which peaks P_1, P_2 and P_3 overlap, MC is distributed more homogeneously than in IN-100. Thus, we may deduce that the MC carbides disperse homogeneously in the alloys when they form at near the peak temperature of P_1.

The most nickel-base superalloys contain transition elements which form MC. The properties of MC affect strongly the mechanical properties of superalloys. Therefore, the present experimental results and also a relationship between the metallic radius and the free energy of formation for MC will be useful for the design of superalloys.

5. Conclusions

The effect of transition elements on the properties of MC carbide in the IN-100 was investigated by means of the DTA, SEM observation and X-ray microanalysis. The following conclusions were obtained.

1. The MC formed in IN-100 was as follows: either TiC with an octahedral shape or $(Ti_{0.80}Mo_{0.17}V_{0.03})C$ with a lattice-like and flaky shape. No detectable amount of nitrogen was found in these carbides.
2. The niobium-, tantalum-, and tungsten-doping changed remarkably the composition of MC in IN-100, but the chromium-, vanadium-, molybdenum-, zirconium-, and hafnium-doping resulted in little or no change in the composition of MC in IN-100. However, in addition to TiC and (Ti, Mo, V) C, zirconium- and hafnium-rich MCs with a serrated-arrow-like shape were found in the zirconium- and hafnium-doped alloy, respectively.
3. The results with respect to MC-composition in the doped alloys were explained by the metallic radius of M in MC and the free energy of MC formation.
4. The morphology and distribution of MC in doped alloys were predicted to some extent by using the DTA profiles.

Acknowledgements

The authors are indebted to Dr M. Morinaga for his helpful discussions. This investigation was supported by the Grant-in-Aid for Scientific Research of the Ministry of Education, Science and Culture, Japan.

References

1. P. S. KOTVAL, J. D. VENABLES and R. W. CALDER, *Met. Trans.* **3** (1972) 453.
2. C. LUND and J. F. RADAVICH, Proceedings of the 4th International Symposium on Superalloys (American Society for Metals, Metals Park, Ohio, 1980) p. 85.
3. G. R. LEVERANT and M. GELL, *Trans. Met. Soc. AIME* **245** (1969) 1167.

4. B. J. PIEARCEY and R. W. SMASHEY, *Trans. AIME* **239** (1976) 451.
5. W. J. BOESH and H. B. CANADA, *J. Met.* **20** (1968) 46.
6. H. E. COLLINS and R. J. QUIGG, *Trans. ASM* **61** (1968) 139.
7. H. E. COLLINS, *ibid.* **62** (1969) 82.
8. M. RAGHAVANT, R. P. MUELLER, C. K. KLEIN and G. A. VAUGHAN, *Scripta Metall.* **17** (1983) 1189.
9. R. F. DECKER, Proceedings of Steel Strengthening Mechanism Symposium, Zurich, Switzerland, 5–6 May (Climax Molybdenum Co., 1969) pp. 1–24.
10. N. YUKAWA, Y. MURATA and T. NODA, Proceedings of the 5th International Symposium on Superalloys (Metallurgical Society of AIME, 1984) p. 83.
11. T. B. REED and E. R. POLLARD, *J. Crystal Growth* **2** (1968) 243.
12. P. VIATOUR, D. COUTSOURADIS, L. HABRAKEN and J. M. DRAPIER, in "High Temperature Alloys for Gas Turbine", edited by D. Coutsouradis, P. Felix, H. Fishmeister, L. Habraken, Y. Lindblom and M. O. Speidel (Applied Science, London, 1978) p. 875.
13. Y. MURATA and N. YUKAWA, *Scripta Metall.* **20** (5) (1986) in press.
14. S. C. FEGAN, T. Z. KATTAMIS and J. E. MORRAL, *J. Mater. Sci.* **10** (1975) 1266.
15. A. K. BHAMBRI, T. Z. KATTAMIS and J. E. MORRAL, *Met. Trans.* **6B** (1975) 523.
16. W. V. YOUDELIS and O. KWON, *Met. Sci.* **17** (1983) 385.
17. S. T. WLODEK, *Trans. ASM* **57** (1964) 110.
18. E. T. TEATUM, K. A. GSHNEIDER Jr and J. T. WABER, LA-2345, US Department of Commerce, Washington, DC (1968) p. 11.
19. R. HULTGREN, P. D. DESAI, D. T. HAWKINS, M. GLEISER and K. K. KELLEY, "Selected Values of the Thermodynamic Properties of Binary Alloys" (American Society for Metals, Metals Park, Ohio, 1973).
20. L. C. BROWNING and P. H. EMMETT, *J. Amer. Chem. Soc.* **74** (1952) 4773.
21. C. P. KEMPTER, *ibid.* **78** (1956) 6209.
22. E. K. STORMS, "The Refractory Carbides" (Academic Press, New York, 1967) p. 6.
23. M. MORINAGA, N. YUKAWA and H. ADACHI, *J. Phys. Soc. Jpn.* **53** (1984) 643.
24. M. HANSEN, "Constitution of Binary Alloy", 2nd Edn (McGraw-Hill, New York, 1958) pp. 1019, 1222.
25. M. HANSEN, E. L. KAMEN, H. D. KESSHER and D. J. McPHERSON, *AIME* **191** (1951) 881.
26. E. RUDY, Technical Report AFML-TR-69-117, Part I (Air Force Materials Laboratory, Wright-Patterson Air Force Base, Ohio, 1970).

Received 21 October
and accepted 20 December 1985